Molecular Therapy
Original Article

Specific Inhibition of Hepatic Lactate Dehydrogenase Reduces Oxalate Production in Mouse Models of Primary Hyperoxaluria

Chengjung Lai,[1] Natalie Pursell,[1] Jessica Gierut,[1] Utsav Saxena,[1] Wei Zhou,[1] Michael Dills,[1] Rohan Diwanji,[1] Chaitali Dutta,[1] Martin Koser,[1] Naim Nazef,[1] Rachel Storr,[1] Boyoung Kim,[1] Cristina Martin-Higueras,[2] Eduardo Salido,[2] Weimin Wang,[1] Marc Abrams,[1] Henryk Dudek,[1] and Bob D. Brown[1]

[1]Dicerna Pharmaceuticals, Inc., Cambridge, MA 02140, USA; [2]Hospital Universitario de Canarias, Centre for Biomedical Research on Rare Diseases (CIBERER), Universidad La Laguna, Tenerife, Spain

Primary hyperoxalurias (PHs) are autosomal recessive disorders caused by the overproduction of oxalate leading to calcium oxalate precipitation in the kidney and eventually to end-stage renal disease. One promising strategy to treat PHs is to reduce the hepatic production of oxalate through substrate reduction therapy by inhibiting liver-specific glycolate oxidase (GO), which controls the conversion of glycolate to glyoxylate, the proposed main precursor to oxalate. Alternatively, diminishing the amount of hepatic lactate dehydrogenase (LDH) expression, the proposed key enzyme responsible for converting glyoxylate to oxalate, should directly prevent the accumulation of oxalate in PH patients. Using RNAi, we provide the first *in vivo* evidence in mammals to support LDH as the key enzyme responsible for converting glyoxylate to oxalate. In addition, we demonstrate that reduction of hepatic LDH achieves efficient oxalate reduction and prevents calcium oxalate crystal deposition in genetically engineered mouse models of PH types 1 (PH1) and 2 (PH2), as well as in chemically induced PH mouse models. Repression of hepatic LDH in mice did not cause any acute elevation of circulating liver enzymes, lactate acidosis, or exertional myopathy, suggesting further evaluation of liver-specific inhibition of LDH as a potential approach for treating PH1 and PH2 is warranted.

INTRODUCTION

The primary hyperoxalurias (PHs) are a group of autosomal recessive disorders caused by the overproduction of oxalate. Oxalate is an end product of glyoxylate metabolism that is mainly produced in the liver and excreted almost entirely by the kidney. Overproduction of oxalate causes precipitation of highly insoluble calcium oxalate (CaOx) crystals in the kidney, resulting in urolithiasis, nephrocalcinosis, and eventually renal failure. As PH patients progress to end-stage renal disease (ESRD), systemic oxalosis (oxalate deposited in all tissues) often occurs as a result of the combination of overproduction and limited excretion of oxalate. There are three forms of PH in which the underlying genetic defects have been identified, designated as PH types 1 (PH1), 2 (PH2), and 3 (PH3). PH1, caused by mutations in the *AGXT* gene, leads to impaired activity of the peroxisomal enzyme alanine:glyoxylate aminotransferase (AGT), while PH2 and PH3 are caused by mutations in the *GRHPR* (glyoxylate reductase/hydroxypyruvate reductase) gene and *HOGA1* (4-hydroxy-2-oxoglutarate aldolase 1) gene, respectively. AGT and GRHPR both play central roles in metabolizing glyoxylate, which is generated from glycolate, glycine, and hydroxyproline metabolism in the liver (Figure 1A). Glyoxylate is converted into either glycine by AGT, glycolate by GRHPR, or oxalate by lactate dehydrogenase (LDH; encoded by the *LDHA* gene in the liver). Reduced AGT or GRHPR activity leads to an increased accumulation of glyoxylate and a subsequent over-production of oxalate.[1–10]

Current treatments for PH1 focus on preserving renal function by decreasing urinary oxalate concentration and CaOx crystallization through increased fluid intake, intensive dialysis, or oral administration of oxalate crystal inhibitors. Additionally, in some patients with PH1, pyridoxine may reduce urinary oxalate excretion. However, these treatments are insufficient, as progressive nephrocalcinosis eventually leads to ESRD in most PH1 patients, where a combined liver and kidney transplant is the only life-saving option.[1,2,4,8,9] Although generally less severe than PH1, there are also no effective treatments for other forms of PH.[7,11]

LDH is an ideal target for reducing hepatic oxalate production because it is the proposed key enzyme responsible for converting glyoxylate to oxalate in the cytoplasm, the last step of oxalate metabolism in liver.[12–15] LDH is an enzyme found in nearly all cell types where it regulates the homeostasis of lactate and pyruvate as well as glyoxylate and oxalate metabolism. Functional LDH is composed of

Received 18 February 2018; accepted 21 May 2018;
https://doi.org/10.1016/j.ymthe.2018.05.016.

Correspondence: Chengjung Lai, Dicerna Pharmaceuticals, Inc., 87 Cambridgepark Drive, Cambridge, MA 02140, USA.
E-mail: clai@dicerna.com
Correspondence: Bob D. Brown, Dicerna Pharmaceuticals, Inc., 87 Cambridgepark Drive, Cambridge, MA 02140, USA.
E-mail: bbrown@dicerna.com

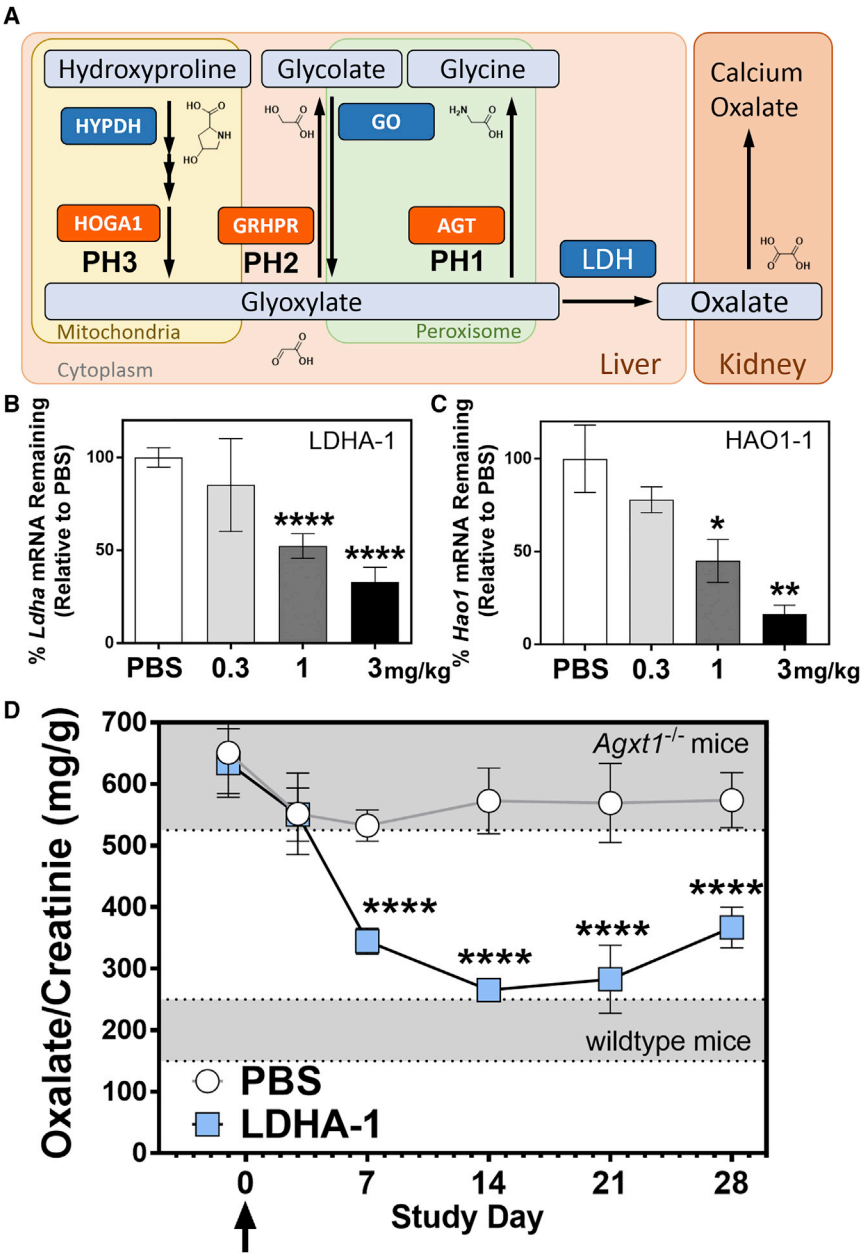

Figure 1. Identification of siRNAs Targeting *Ldha* or *Hao1* for Study of PH

(A) Oxalate metabolism pathway overview. (B) siRNA targeting *Ldha* conjugated to GalNAc residues for ligand-mediated targeting specifically to hepatocytes (designated as LDHA-1) through subcutaneous injection has an ED_{50} of approximately 1.6 mg/kg in wild-type mice (see also Figure S1). (C) siRNA targeting *Hao1* conjugated to GalNAc residues for ligand-mediated targeting specifically to hepatocytes (designated as HAO1-1) through subcutaneous injection has an ED_{50} of approximately 1.0 mg/kg in wild-type mice (see also Figure S1). Data are presented as mean ± SD. Unpaired t test for statistical significance relative to PBS treatment group at each dose level. (D) Male *Agxt1*$^{-/-}$ mice were subcutaneously injected with 5 mg/kg of LDHA-1 or PBS at a single dose (n = 5). Urine samples were collected weekly and analyzed for oxalate (with LC/MS) and creatinine levels. Ranges of urinary oxalate levels in wild-type and *Agxt1*$^{-/-}$ mice are indicated. Data are presented as mean ± SD. Unpaired t test for statistical significance relative to PBS treatment group at each time point. *p < 0.05; **p < 0.01; ****p < 0.0001. AGT, alanine-glyoxylate aminotransferase; GO, glyoxylate oxidase; GRHPR, glyoxylate reductase/hydroxypyruvate reductase; HAO1, hydroxyacid oxidase 1; HOGA1, 4-hydroxy-2-oxoglutarate aldolase 1; HYPDH, hydroxyproline dehydrogenase; LDH, lactate dehydrogenase.

four polypeptide chains to form a tetramer. The two most common subunits, known as muscle (M) or heart (H) forms of LDH, are encoded by *LDHA* and *LDHB* genes, respectively. Five different isozymes (LDH1 through LDH5) have been identified based on their subunit composition (4H, 3H1M, 2H2M, 1H3M, 4M), and the major isozyme of liver and skeletal muscle, LDH5, has 4M subunits.[16,17]

Although LDH controls the interconversion of pyruvate and lactate in the liver and other tissues, reported patients who completely lack the LDH M-subunit do not exhibit any compromised liver functions.[18–23] The absence of any liver-specific phenotype in *LDHA*-deficient patients and the direct role of LDH in controlling the ultimate step of oxalate production prompted us to evaluate whether liver-specific *LDHA* inhibition is an effective approach for treating PHs using animal models. We and others have previously demonstrated in animal models that RNAi targeting the glycolate oxidase (GO) enzyme is a novel strategy for treating PH1.[24,25]

In this study, we show that hepatic LDH is an efficient target for reducing oxalate production in animal models of PH1 and PH2, as well as mouse models of chemically induced hyperoxaluria. Administration of *LDHA* RNAi conjugate achieves potent and durable reduction of LDH protein and enzyme activity in mice and non-human primates (NHPs). In addition, we demonstrate that specific inhibition of hepatic LDH is sufficient to significantly reduce urinary oxalate in a hyperoxaluria-prone environment where GO enzyme retains full functionality. Together, our results provide the first *in vivo* evidence that supports the physiological role of hepatic LDH as the main enzyme for oxalate production.

RESULTS

We and others have previously demonstrated that inhibition of GO with small interfering RNAs (siRNAs) delivered by lipid

nanoparticle (LNP) reduces urinary oxalate levels in mouse models of PH1.[24–27] To evaluate LDH as an efficient target for the treatment of PH because of its proposed role in the final step of oxalate production, we compared the relationship between oxalate reduction and target protein inhibition following RNAi-mediated silencing of *Ldha* or *Hao1* (the gene encoding GO) in PH1, PH2, and chemically induced hyperoxaluria mouse models.

siRNAs Targeting *Ldha* Effectively Reduce Hepatic LDH Expression and Urinary Oxalate Concentrations in the *Agxt1*$^{-/-}$ PH1 Mouse Model

Potent siRNAs against *Ldha* and *Hao1* were conjugated with *N*-acetylgalactosamine (GalNAc) residues for ligand-mediated targeting specifically to hepatocytes (designated as LDHA-1 and HAO1-1). The activity of LDHA-1 and HAO1-1 was confirmed in wild-type mice with a median effective dose (ED_{50}) of approximately 1.6 and 1.0 mg/kg, respectively (Figures 1B and 1C; Figure S1). Reduction of LDH levels also reduced urinary oxalate concentrations from approximately 570 to 260 mg/g (normalized with creatinine) in *Agxt1*$^{-/-}$ mice injected with a single 5 mg/kg dose of LDHA-1 (Figure 1D). These results confirm an important role for hepatic LDH in oxalate production in a mammalian disease model of PH type I.

Reduction of Hepatic LDH Protects Against Kidney Damage Elicited by EG in *Agxt1*$^{-/-}$ Mice

Male *Agxt1*$^{-/-}$ mice develop variable degrees of kidney CaOx deposits when fed ethylene glycol (EG),[24,26] a precursor of glycolate, where GO inhibition is sufficient to prevent the damage.[24] To determine whether the reduction of oxalate production by inhibition of hepatic LDH is sufficient to prevent kidney damage, male *Agxt1*$^{-/-}$ mice were given free access to drinking water containing EG while being subjected to weekly treatments with LDHA-1. EG feeding resulted in an increase in urinary oxalate concentrations to more than 1,000 mg/g (normalized with creatinine), which was significantly inhibited by treatment with LDHA-1 (Figures 2A and 2B). Continued suppression of LDH protein with eight weekly doses of LDHA-1 reduced urinary oxalate levels to approximately 260 mg/g, which is near the baseline levels of wild-type mice (Figure 2A). Histological characterization of kidney tissue shows variable degrees of kidney CaOx deposits in control mice that were effectively blocked with LDHA-1 treatment (Figure 2B; Figure S2). These results demonstrate that utilizing LDHA-1 to reduce hepatic LDH expression is sufficient to protect against kidney CaOx deposition and prevent hyperoxaluria in a prolonged and aggravated oxalate-producing environment, thus preventing kidney damage in PH type I.

Hepatic LDH Silencing Efficiently Reduces Oxalate in the *Agxt1*$^{-/-}$ PH1 Mouse Model

A role for GO in converting glyoxylate to oxalate has been proposed;[8,12–14,25] however, it has not been extensively evaluated experimentally. Using purified human recombinant enzyme, it was suggested that GO does not play a major role in converting glyoxylate to oxalate.[12] However, to our knowledge, there have not been any *in vivo* studies in mammalian systems investigating the role of GO on glyoxylate-to-oxalate conversion. It is important to understand whether other enzymes also are involved in glyoxylate-to-oxalate conversion, in order to fully value the therapeutic potential of targeting hepatic LDH. If there were other hepatic enzymes that can also convert glyoxylate to oxalate, then inhibiting LDH will not be sufficient to reduce oxalate production significantly, especially in an environment with elevated levels of glycolate or glyoxylate, as presumably occurs in hepatocytes of PH patients. To better understand this, we compared the effect of targeting LDH versus GO in a PH1 mouse model. LDHA-1 and HAO1-1 were subcutaneously (s.c.) injected into male *Agxt1*$^{-/-}$ mice at varying doses, which were chosen to achieve a broad range of comparable levels of target protein inhibition (Figure 3). Notably, we observed a disproportionate correlation between GO protein suppression and urinary oxalate reduction in mice treated with HAO1-1 (Figures 3A, 3C, and 3D). While mice treated with LDHA-1 showed a meaningful reduction of urinary oxalate levels even at siRNA dose levels resulting in less than 50% reduction of LDH protein expression (Figures 3A, 3B, and 3D), greater reduction of GO protein compared with LDH was required to elicit an effect on oxalate reduction. These results support that LDH and GO play distinct roles in the glyoxylate and oxalate metabolic pathways. Similarly, this was further confirmed by a disproportionate relationship between GO protein repression and the accumulation of glycolate following HAO1-1 treatment (Figure S3). We do not yet fully understand the mechanisms that contribute to the disproportionate relationship between GO protein repression and oxalate reduction; these results support that a critical level of GO silencing is necessary to achieve a meaningful reduction of urinary oxalate concentrations while reduction of LDH and urinary oxalate are directly related. Regardless of whether this disproportionate relationship is simply due to an excess amount of GO enzyme in the liver or due to metabolic adaptability, these results suggest a key and unique role of hepatic LDH in oxalate production and further support the therapeutic targeting of hepatic LDH to achieve oxalate reduction in PH1.

GO Reduction Induces Glycolate Accumulation in a Disproportionate Manner in NHPs

To investigate whether the disproportionate relationship between GO reduction and glycolate accumulation is common across species, we examined the relationship between GO protein suppression and plasma glycolate accumulation in NHPs. Repeat dosing of cynomolgus monkeys with HAO1-1 significantly reduced *HAO1* mRNA and GO protein levels in NHPs (Figures 4A and 4B). Following treatment with HAO1-1, we observed an increase in plasma glycolate levels that corresponded to the HAO1-1 dose level and dosing frequency (Figure 4A). We also observed that the subsequent reversal of elevated plasma glycolate occurred more rapidly than recovery of GO protein expression following the final dose of HAO1-1 (Figure 4A). For example, at study week 19, GO protein remained substantially repressed while plasma glycolate levels had declined back to near-baseline levels (Figure 4A). Particularly, for animals receiving 2 mg/kg doses every 2 weeks, plasma glycolate levels were significantly

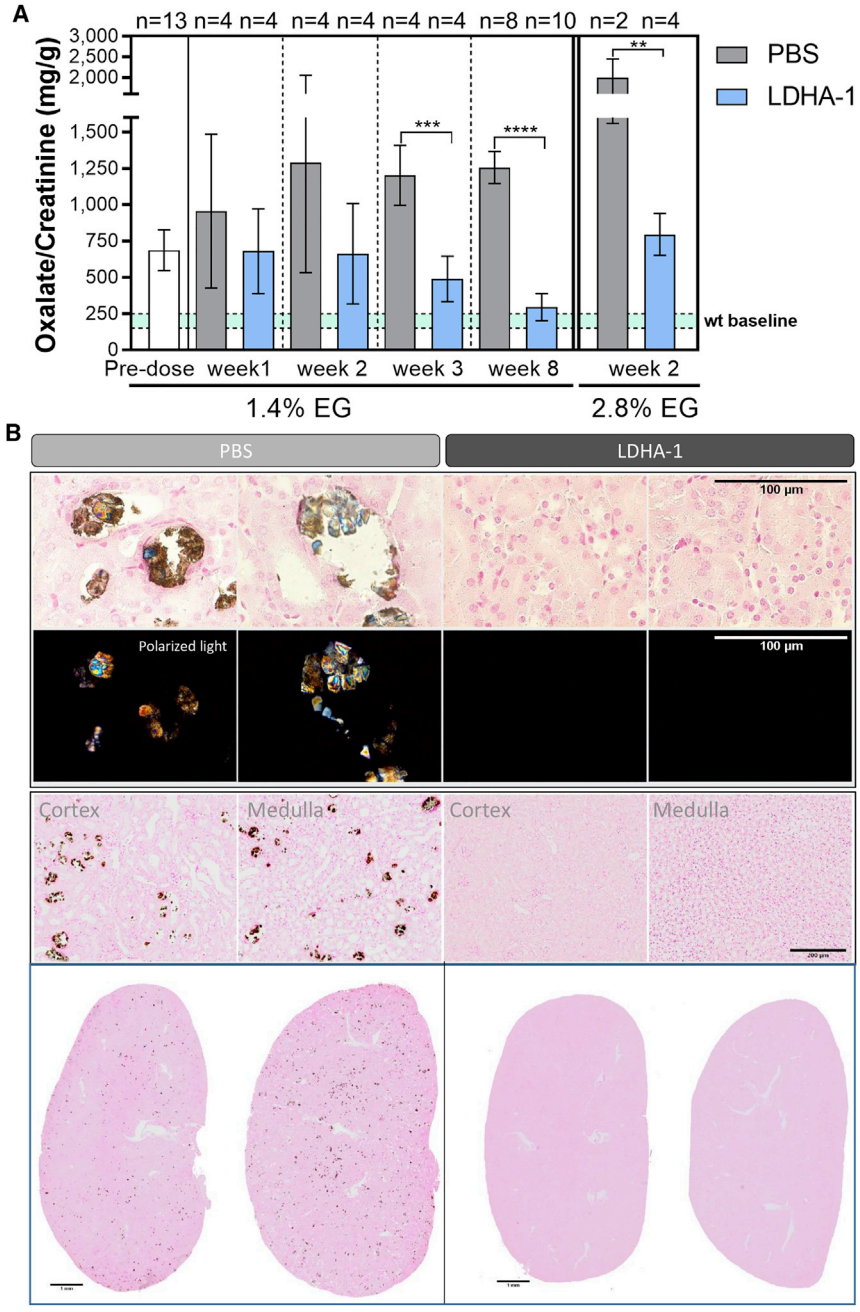

Figure 2. LDHA-1 Prevents EG-Induced Calcium Oxalate Deposition in a PH1 Mouse Model

Male *Agxt1*$^{-/-}$ mice were given free access to 1.4% or 2.8% EG in their drinking water and subcutaneously injected with 5 mg/kg of LDHA-1 weekly. Urine samples were collected using metabolic cages and analyzed for oxalate and creatinine levels. Mice fed 1.4% EG for 8 weeks were sacrificed, and the kidneys were collected for the evaluation of CaOx crystals on week 8. (A) Urinary oxalate levels of EG-fed mice treated with PBS or LDHA-1. Data are presented as mean ± SD. Unpaired t test for statistical significance relative to PBS treatment group at each time point. **$p < 0.01$; ***$p < 0.001$; ****$p < 0.0001$. wt, wild-type mouse urinary oxalate levels. (B) Histological analysis of kidney tissue was performed to detect CaOx crystals using Pizzolato's staining. Representative images demonstrate how control-treated mice developed CaOx crystals that exhibited characteristic birefringence with polarized light and positive staining using the Pizzolato's method for CaOx. EG-fed mice in the control group displayed variable CaOx depositions. Representative sections from animals of the PBS group with the most severe damage are shown here. Additional images and quantitative analysis of kidney sections can be found in Figure S2. Scale bars represent 100 µm (first and second rows), 200 µm (third row), or 1 mm (bottom row).

reduced to near-baseline levels between weeks 15 and 19 ($p < 0.05$), during which time GO protein suppression was maintained (Figure 4A). This disproportionate relationship between GO protein repression and glycolate accumulation was further emphasized when GO protein and plasma glycolate levels for individual animals were compared (Figure 4C). Taken together, these results suggest that LDH and GO play distinct roles in the glyoxylate and oxalate metabolic pathways in both rodent and NHP hepatocytes. To better determine the therapeutic potential of targeting hepatic LDH, we continued to characterize and compare the roles of LDH and GO in oxalate production in genetically engineered or chemically induced animal models of PH.

Hepatic LDH, but Not GO, Plays a Direct Physiological Role in Oxalate Production

To thoroughly scrutinize the physiological roles of GO and LDH in glyoxylate-to-oxalate conversion, we deliberately created a potential hyperoxaluric condition in mice through the combination of gene knockdown and EG precursor feeding as a way to further increase the hypothetical glyoxylate pool. *Agxt1*$^{-/-}$ mice were treated weekly with both GRHPR-1 and LDHA-1 while retaining fully functional GO enzyme. In these mice, hepatic AGT and GRHPR were reduced, and the conversion of glyoxylate to glycine or glycolate, respectively, should be limited. Assuming glyoxylate is the main precursor of oxalate, our observation of high initial levels of oxalate in these animals suggests that excess levels of glyoxylate should be available in this condition to be converted into oxalate by LDH and GO, if GO plays a role in glyoxylate-to-oxalate conversion. siRNA-mediated inhibition of hepatic LDH would not be sufficient to prevent hyperoxaluria if GO were also able to efficiently convert excess glyoxylate into oxalate. We observed that, in the presence or absence of EG, reduction of LDH was able to continually reduce

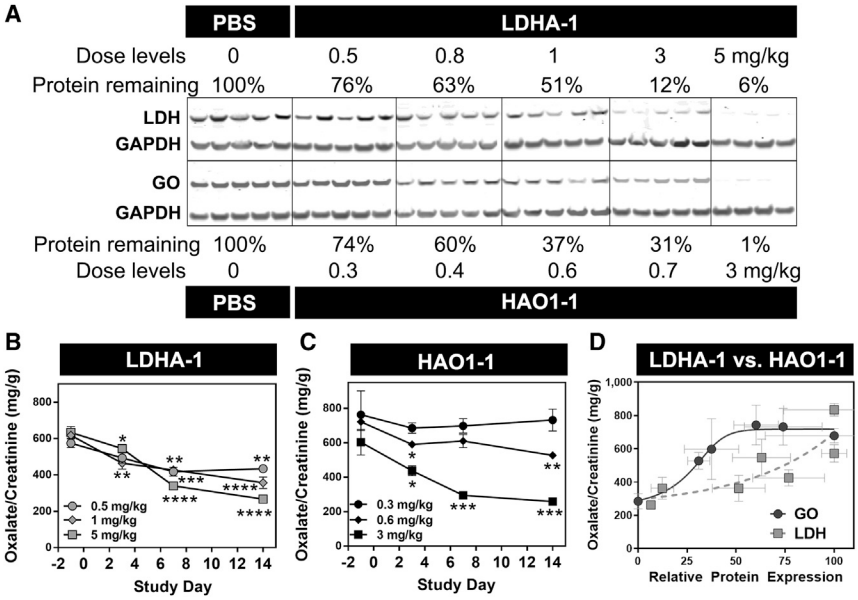

Figure 3. Inhibition of Hepatic LDH and GO Reduces Urinary Oxalate in a PH1 Mouse Model

The lead *Hao1* and *Ldha* siRNA conjugates designated as HAO1-1 and LDHA-1, respectively, were subcutaneously injected into male *Agxt1*$^{-/-}$ mice at a single dose of 0.3, 0.4, 0.6, 0.7, or 3 mg/kg (HAO1-1) or 0.5, 0.8, 1, 3, or 5 mg/kg (LDHA-1). (A) Results of western blot analysis on the effect of HAO1-1 and LDHA-1 on target protein, GO and LDH, respectively, at selected dose levels. The relative protein expression levels in the livers of four to five animals per group compared with the PBS group are shown for each dose level, and the dose levels were indicated. Each lane represents an individual animal of each group. LC/MS analysis (mean ± SD) of urinary oxalate levels in (B) LDHA-1- and (C) HAO1-1-treated *Agxt1*$^{-/-}$ mice. (D) Portions of animals receiving LDHA-1 or HAO1-1 at different dose levels (n = 5 for each group) were euthanized and analyzed for their relative target protein expression (mean ± SD) in the livers at day 10 compared with their urinary oxalate levels normalized to creatinine (mean ± SD) at day 14. Days 10 and 14 represent the nadir of protein and oxalate reduction, respectively. One-way ANOVA test for statistical significance relative to pre-dose. *p < 0.05; **p < 0.01; ***p < 0.001; ****p < 0.0001.

urinary oxalate levels in an environment with presumably high levels of glyoxylate while maintaining fully functional GO enzyme (Figure 5A). As predicted, urinary glycolate levels were reduced over time as a result of functional GO enzyme converting glycolate to glyoxylate (Figure 5B). These results further support that there is only one key enzyme, LDH, that catalyzes the conversion of glyoxylate to oxalate even in an environment with excess upstream precursors available from endogenous or exogenous sources.

Targeting Hepatic LDH Reduces Urinary Oxalate Levels in a *Grhpr*$^{-/-}$ PH2 Mouse Model

To further evaluate the therapeutic role of hepatic LDH in PH, we employed a genetically engineered murine model of PH2. *Grhpr*$^{-/-}$ mice carry a germline null mutation in the gene encoding GRHPR, resulting in a higher baseline of urinary oxalate levels compared with their wild-type counterparts.[28] *Grhpr*$^{-/-}$ animals were treated weekly with LDHA-1, and urinary oxalate levels were assessed. Levels of urinary oxalate were reduced after LDHA-1, but not HAO1-1, treatment (Figure 6A). Similarly, oxalate excretion rates over a period of 24 hr were also reduced with LDHA-1 compared with HAO1-1 treatment (Figure S4). We then further confirmed that LDH, but not GO, suppression causes the reduction of urinary oxalate levels in a *Grhpr*-knockdown PH2 mouse model, a model that represents PH2 patients who have residual GRHPR enzyme remaining in hepatocytes. A similar window of oxalate elevation was observed in the *Grhpr*-knockdown PH2 mice compared with *Grhpr*$^{-/-}$ mice. Similarly, LDH reduction was able to prevent oxalate elevation in *Grhpr*-knockdown mice while suppression of neither GO nor hydroxyproline dehydrogenase (HYPDH) protein expression showed an effect on urinary oxalate levels (Figure 6B). Less than 10% of baseline levels of target genes remained after siRNA treatment (Figure S5), further confirming that the observed differences in reduction of urinary oxalate levels are specific to the distinct roles of GO, HYPDH, and LDH in glyoxylate and oxalate metabolism. Taken together, our results imply that targeting LDH, rather than GO, can be an effective approach for treating PH2.

Inhibition of LDH Reduces Urinary Oxalate Levels in EG- and Hydroxyproline-Induced Models of Hyperoxaluria

We utilized low concentrations of EG and hydroxyproline feeding as chemically induced mouse models for investigating the roles of LDH in oxalate production under hyperoxaluric conditions in mice without mutations in AGT or GRHPR. Wild-type mice were provided free access to 0.7% EG in their drinking water and injected weekly with LDHA-1 or HAO1-1. EG-fed mice showed a gradual elevation of urinary oxalate levels that peaked between 4 and 6 weeks despite sufficient GO reduction (Figures 6C and 6D; Figure S6). In contrast, LDHA-1 treatment reduced urinary oxalate to near-baseline levels (Figure 6C). Moreover, LDHA-1 treatment reduced urinary oxalate levels to near-baseline levels in *Grhpr*-knockdown PH2 mice simultaneously fed with EG (Figure 6E). Wild-type mice pre-treated for 2 weeks with LDHA-1 were then given 1% hydroxyproline-containing food for 2 additional weeks, while continuing to receive weekly doses of LDHA-1. Treatment with LDHA-1 significantly reduced urinary oxalate levels to near-baseline levels (Figure 6F). Taken together, these results suggest that hepatic LDH is an efficient target for oxalate reduction in a hyperoxaluric environment not caused by mutations in AGT or GRHPR, and further support its key role in glyoxylate-to-oxalate conversion.

LDHA RNAi Duplex Is Active in NHPs and Chimeric Mice with Humanized Livers

To confirm that our *LDHA* knockdown approach is effective across species, we evaluated inhibition of *LDHA* target mRNA in

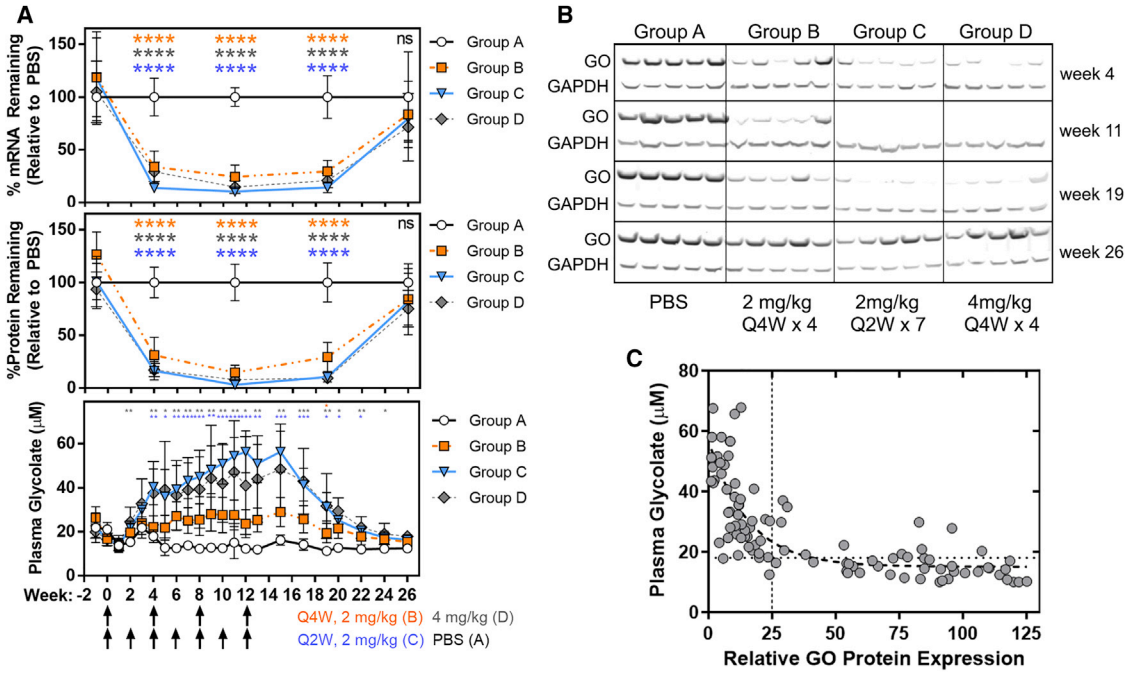

Figure 4. Non-linear Relationship between GO Enzyme Reduction and Glycolate Elevation in NHPs

HAO1-1 or PBS as a control were subcutaneously injected into cynomolgus monkeys at the indicated dose levels and schedules. Liver biopsies were collected for analysis of mRNA and protein at indicated time points. Plasma samples were also collected and analyzed with LC/MS for glycolate levels. Each group contains five animals. Arrows indicate time of injection. (A) Quantitative results of RT-PCR and western blot of *Hao1* mRNA and GO protein following treatment with HAO1-1. LC/MS analysis of plasma glycolate with PBS or HAO1-1 treatment. (B) Western blot analysis that was used for the quantification results shown on (A). (C) Individual animals were analyzed for their GO protein expression and plasma glycolate levels at weeks 4, 11, 19, and 26. Data are presented as mean ± SD. One-way ANOVA test for statistical significance relative to PBS treatment group at each time point. *$p < 0.05$; **$p < 0.01$; ***$p < 0.001$; ****$p < 0.0001$. ns, non-significant; Q2W, once every 2 weeks, Q4W, once every 4 weeks.

NHPs and in chimeric mice with human hepatocyte replacement of their livers. An NHP- and human-specific *LDHA* siRNA, designated as LDHA-2, was identified and evaluated in cynomolgus monkeys and chimeric mice. LDHA-2 was s.c. injected into cynomolgus monkeys with different regimens (Figure 7). Liver biopsies were collected at varying time points and analyzed for target mRNA and protein levels, as well as the enzymatic activity of LDH. We demonstrated that LDHA-2 potently suppressed *LDHA* mRNA expression, resulting in a significant reduction of LDH protein with more than 50% of inhibition sustained for 8 weeks after the final dose (Figures 7A–7C). Furthermore, LDH activity in liver extracts prepared from treated NHPs was reduced with LDHA-2 treatment (Figure 7D). PXB mice are chimeric mice on an immunocompromised genetic background with a humanized liver that is highly repopulated by human hepatocytes.[29] In this study, chimeric mice were estimated to have around 80% of the liver repopulated with human hepatocytes based on circulating human-albumin levels. Similarly, we demonstrated that LDHA-2 achieved specific inhibition of human *LDHA* mRNA in chimeric mice containing human hepatocytes (Figure 7E).[29] LDHA-2 displayed expected target delivery and gene suppression in monkey and human hepatocytes, suggesting our approach is translatable across species.

Liver-Specific Inhibition of LDH Exhibits No Acute Lactic Acidosis or Liver Toxicity in Mice

In addition to its role in oxalate production, LDH regulates the systemic balance of pyruvate and lactate levels in the body. In this process, referred to as the Cori cycle, lactate produced in the muscle or other organs during anaerobic glycolysis is transferred to the liver and kidney for conversion to pyruvate by LDH for subsequent gluconeogenesis (Figure S7).[30] One potential side effect for liver-specific downregulation of *LDHA* could be the accumulation of circulating lactate. In order to understand the possible development of lactate acidosis following liver-specific *LDHA* knockdown, we treated wild-type and *Agxt1*$^{-/-}$ mice weekly with high-dose levels of LDHA-1 for 6 weeks. Notably, no elevation of plasma lactate level, weight loss, or evidence of liver toxicity was detected in wild-type or *Agxt1*$^{-/-}$ mice at any dose level (Figure 8; Figures S8 and S9). Also, in this short-term study, LDHA-1 treatment inhibited *Ldha* expression only in the liver and not in the kidney, muscle, skin, or uterus, where *Ldha* inhibition might affect their normal function (Figure 8E). These results illustrate that liver-specific *LDHA* knockdown using an RNAi approach does not cause any acute effects on lactate homeostasis or acute liver toxicity in mice.

Collectively, our data demonstrate that liver-specific knockdown of *LDHA* results in potent and durable target inhibition in diseased

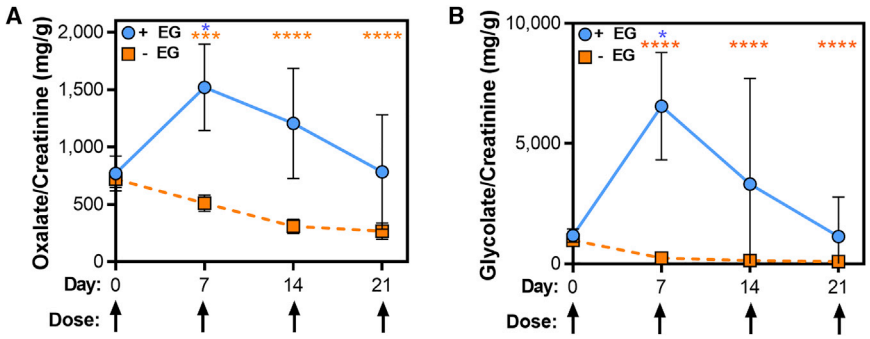

Figure 5. Targeting Hepatic LDH Reduces Oxalate Production in AGXT- and GRHPR-Deficient Mice Fed with EG

Male *Agxt1*$^{-/-}$ mice were subcutaneously injected weekly with siRNA conjugates targeting both *Grhpr* and *Ldha*, GRHPR-1 (10 mg/kg) and LDHA-1 (5 mg/kg), respectively, in the presence (blue circle, n = 5) or absence (orange square, n = 10) of 0.7% EG. Urine samples were collected for the analysis of urinary (A) oxalate and (B) glycolate levels by an LC/MS method. Data are presented as mean ± SD. One-way ANOVA test for statistical significance relative to pre-dose. *p < 0.05; ***p < 0.001; ****p < 0.0001.

mice, mice with humanized livers, and NHPs, suggesting a common molecular mechanism of target inhibition across species.

DISCUSSION

In this study, we established the pivotal role of LDH in oxalate production and its subsequent urinary excretion in several models of PH. Liver-specific suppression of *Ldha* mRNA expression efficiently reduces hepatic LDH enzyme in wild-type and PH1 mice, as well as urinary oxalate levels in all assessed hyperoxaluria animal models. siRNAs designed to specifically target hepatocytes also avoided potential undesired target knockdown in muscle, skin, or uterus in a short-term study in mice.

Potential Differences in the Oxalate Metabolic Pathways and Kidney Physiology Between Mice, Monkeys, and Humans

We demonstrate that inhibition of hepatic LDH is efficient for reducing urinary oxalate levels in several experimental models of hyperoxaluria. Our short-term study of high-dose levels of LDHA-1 treatment also yielded no acute liver toxicity in mice, which agrees with the observed absence of any liver-specific phenotype in *LDHA*-deficient patients.[18–23] However, there are potential differences in the oxalate metabolic pathways, as well as in kidney and general physiology between mice, monkeys, and humans that should be considered. For example, HOGA1 deficiency causes PH3 in humans by an unidentified mechanism, while *Hoga1* deficiency presents with normal urinary oxalate in mice (Figure S10).[31–36] AGT deficiency causes kidney stones in humans, yet frequently fails to induce CaOx deposition in mice without the administration of EG.[26] One of the best studied aspects of AGT is its subcellular localization in various organisms. In mice and rats, AGT is present both in the mitochondria and peroxisomes, while in humans and rabbits, it is exclusively located in the peroxisome.[37] However, there is limited information available regarding the expression level, protein stability, or catalytic activity of AGT enzymes, all of which could contribute to species-specific differences in the AGT-deficient phenotype. Additionally, siRNA-mediated reduction of AGT expression in monkeys did not induce hyperoxaluria as it does in the PH1 mouse model and in PH1 patients (Figure S11), further supporting the need for further understanding of species differences in future preclinical and clinical studies.

In an effort to examine other potential therapeutic targets, we found that targeting hepatic HYPDH does not impact oxalate production and does not induce an accumulation of hydroxyproline in a mouse model of PH1 (Figure S12). However, reduction of *Hypdh* expression induced an accumulation of hydroxyproline when high amounts of hydroxyproline were included in the diet (Figure S12). These results suggest that regular turnover of collagen and subsequent hydroxyproline production is not a main source of oxalate in mice, as it is believed to be in humans,[28,36] which poses another potential difference between species.

Interestingly, in all studies we have conducted in wild-type mice or in NHPs with liver-specific suppression of LDH, we have not detected any elevation of glycolate in urine or plasma samples (Figure S13). Male and female *Agxt1*$^{-/-}$ mice treated with LDHA-1 also did not demonstrate any further elevation of glycolate compared with PBS-treated mice (Figure S14). Inhibition of hepatic LDH is predicted to result in an accumulation of glyoxylate that can be converted efficiently to glycolate by GRHPR in PH1. The absence of glycolate elevation with LDH inhibition deserves further exploration.

Evaluation of Potential Metabolic Complications of Inhibition of Hepatic LDH

Patients with hereditary *LDHA* deficiency have been reported to present with exertional myopathy, erythematosquamous skin lesions, and uterine stiffness during pregnancy; however, there are no reports of liver-specific toxicities.[18–23,38,39] An RNAi approach with GalNAc-conjugated siRNAs for liver-specific knockdown of *Ldha* demonstrates in mice that there is no significant knockdown of *Ldha* in muscle, skin, or uterine tissue (Figure 8). We have observed normal lactate production and regular performance during exercise in wild-type mice treated with LDHA-1 (Figure S15), suggesting muscle LDH function was not affected in this study. Another potential concern for liver-specific inhibition of *LDHA* is the possibility of systemic lactic acidosis. Under normal conditions, referred to as the Cori cycle, the liver and kidneys will uptake lactate generated in muscle and other tissues from anaerobic glycolysis for conversion to pyruvate by LDH for subsequent gluconeogenesis.[30] We did not observe any elevation of circulating lactate in wild-type mice, *Agxt1*$^{-/-}$ mice, or NHPs with liver-specific *LDHA* knockdown (Figure 8; Figure S16). One potential explanation for this observation is that residual hepatic LDH or the uninhibited kidney LDH activity may be sufficient for

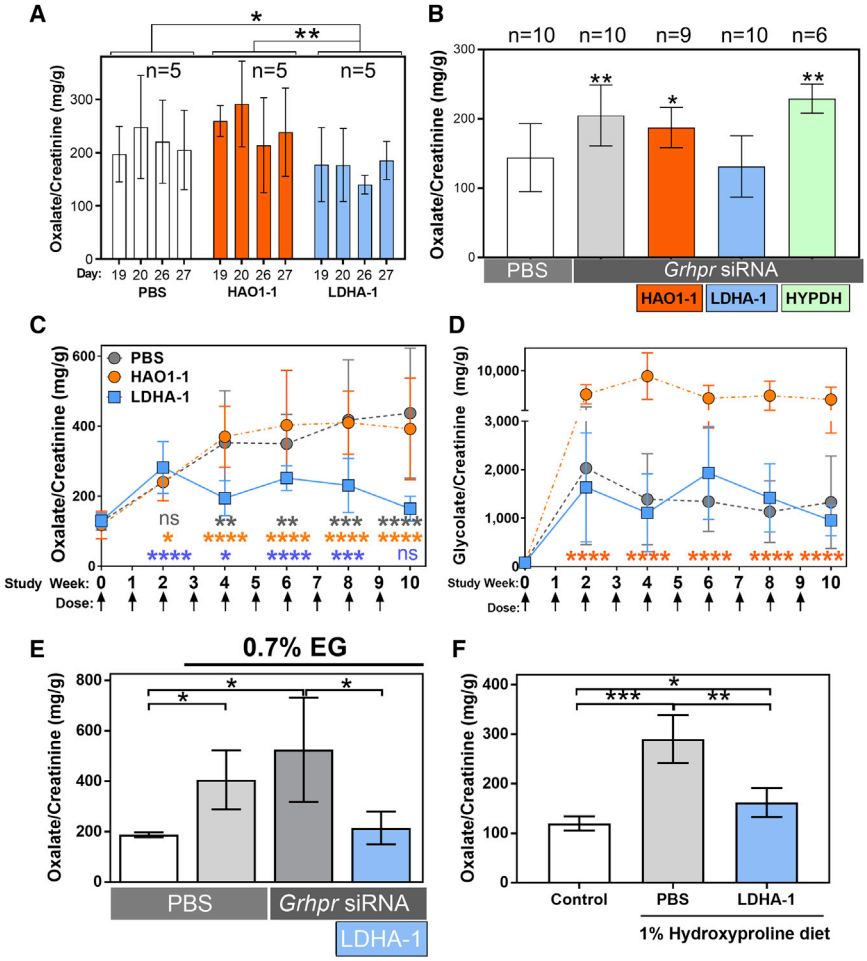

Figure 6. LDHA-1 Reduces Urinary Oxalate Levels in PH2, EG, and Hydroxyproline Mouse Models

(A) Male *Grhpr*$^{-/-}$ mice were subcutaneously injected with PBS as a control compared with HAO1-1 or LDHA-1 at 5 mg/kg weekly (n = 5 for each group). Urine samples were collected on days 19, 20, 26, and 27, and analyzed by enzymatic assay for urinary oxalate and creatinine levels. Data are presented as mean ± SD. Unpaired t test for statistical significance was performed for each group (PBS versus LDHA-1, PBS versus HAO-1, and LDHA-1 versus HAO1-1) using the average of measurements on days 19, 20, 26, and 27. (B) A second PH2 mouse model was generated using an RNAi approach with repeat dosing of a *Grhpr* siRNA formulated in lipid nanoparticle (LNP) at 1 mg/kg every 2 weeks in male C57BL/6 wild-type mice. siRNAs targeting *Hao1* (n = 9), *Ldha* (n = 10), or *Hypdh* (n = 6) formulated in LNP were injected intravenously weekly at 0.3 mg/kg starting on day 20 for 4 weeks. Data are presented as mean ± SD. Unpaired t test for statistical significance relative to PBS treatment group. (C and D) Male C57BL/6 wild-type mice fed 0.7% EG in their drinking water while being given weekly subcutaneous doses of PBS control (n = 10), LDHA-1 (n = 10), or HAO1-1 (n = 10) at 5 mg/kg. LC/MS analysis of urinary oxalate (C) and urinary glycolate (D) levels were compared in treated animals. Urine samples were collected manually. Data are presented as mean ± SD. One-way ANOVA test for statistical significance relative to pre-dose. (E) Male C57BL/6 mice were injected weekly with *Grhpr* siRNA to induce elevation of urinary oxalate of PH2 model in the presence or absence of weekly LDHA-1 treatment. Where indicated, mice were also fed with 0.7% of EG for 4 weeks. LC/MS analysis of urinary oxalate is presented as mean ± SD (n = 5). Unpaired t test for statistical significance relative to control group. (F) Male C57BL/6 mice were injected with LDHA-1 weekly. Concurrent with the third dose, 1% of hydroxyproline was added to their diet. Urine samples were collected at the end of the fourth week for analysis of urinary oxalate levels with LC/MS. Data are presented as mean ± SD (n = 5). Unpaired t test for statistical significance relative to control group. *p < 0.05; **p < 0.01; ***p < 0.001; ****p < 0.0001. ns, non-significant.

completion of the Cori cycle. It is also possible that LDH may exhibit more catalytic efficiency for pyruvate-to-lactate interconversion compared with glyoxylate-to-oxalate conversion; thus, a greater impact from reduction of LDH enzyme will be observed on oxalate production than on lactate homeostasis. However, it is worth noting that LDH enzyme kinetics are highly dependent on the concentrations of lactate and pyruvate, where, at equilibrium, higher amounts of lactate compared to pyruvate are present in the cell. Production of lactate depends on pyruvate, which is a crossroads of glycolysis, glycogenosis, and gluconeogenesis pathways.[40,41]

Due to the role of LDH in the Cori cycle, it is possible that liver-specific deficiency of *LDHA* could also lead to myopathy and other adverse effects because of a potential impact on gluconeogenesis in the liver caused by the reduction of pyruvate production from lactate. Pyruvate serves as one of the key intermediates for gluconeogenesis. We have observed normal muscle performance that was accompanied with increased glycolysis as demonstrated by the transient elevation of pyruvate in LDHA-1-treated mice (Figure S15). These results imply that there is no defect in hepatic gluconeogenesis and glucose resupply from the liver to muscle cells with liver-specific *Ldha* silencing. However, we could not rule out the possibility that rodents employ different pathways to maintain blood glucose than humans. Together, as aforementioned, due to the potential differences in metabolism and physiology between species, future clinical evaluation of liver-specific LDH inhibition as a therapeutic approach is required to fully understand its impact on all relevant metabolic pathways.

In mice, *Ldha* null mutations have been reported to cause either embryonic lethality or hemolytic anemia.[42,43] This phenotypic discrepancy in the severity of *LDHA* deficiency between mice and humans can be attributed to the diverse levels of *LDHB* expression that can compensate for cell respiration function during early embryo development and erythropoiesis across species.[42–44] Regardless of the differences in the

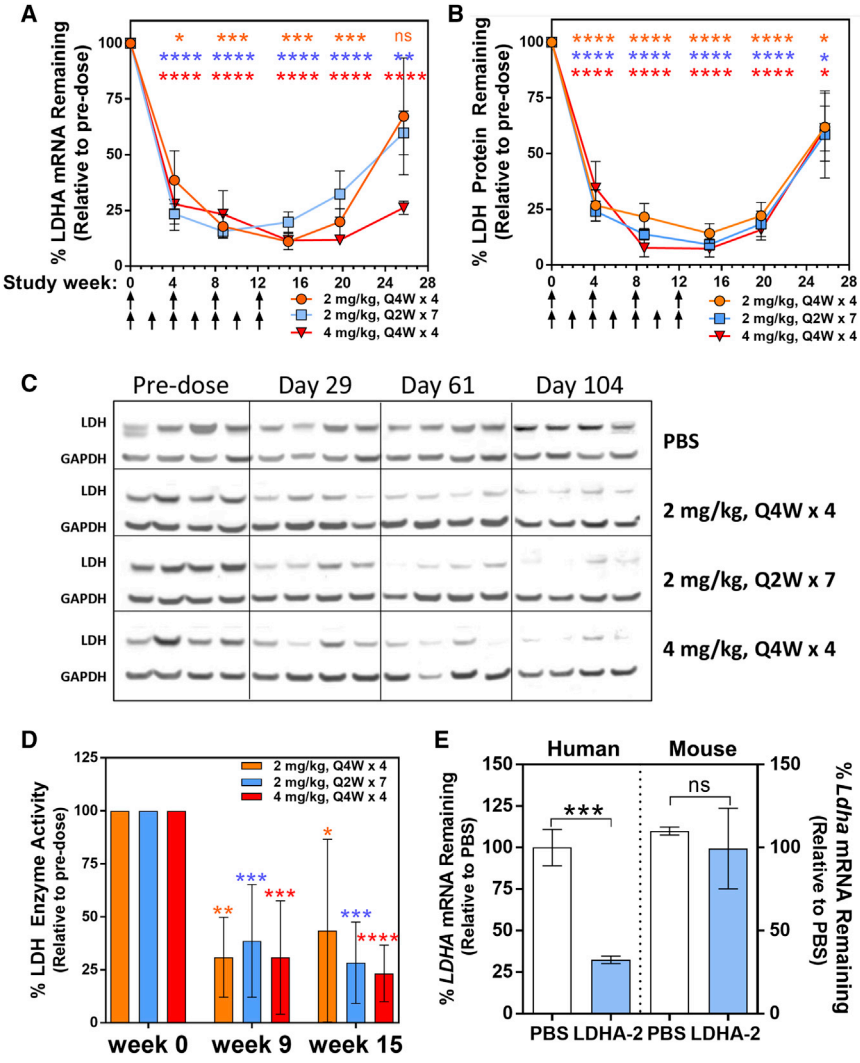

Figure 7. *LDHA* siRNAs Are Active in NHPs and Chimeric Mice with Humanized Livers

An NHP and human-specific *LDHA* siRNA, LDHA-2, was subcutaneously injected into cynomolgus monkeys following the indicated dosing regimens. Liver biopsies were collected for analysis of target mRNA (A) and protein levels (B and C), as well as the enzymatic activity (D), of LDH at the indicated time points. Arrows indicate timing of siRNA injections. (B) Quantitative results of western blot analysis shown in (C). (B–D) Data are presented as mean ± SD. One-way ANOVA test for statistical significance relative to pre-dose. (E) PXB mice with humanized livers were given three weekly injections of 5 mg/kg LDHA-2 (n = 3) or PBS as a control (n = 3). Liver samples were collected 10 days after the final dose for measurement of *LDHA* mRNA repression. RT-PCR analysis were performed using human or mouse-specific primers. Data are presented as mean ± SD (n = 5). Unpaired t test for statistical significance relative to control group. *p < 0.05; **p < 0.01; ***p < 0.001; ****p < 0.0001. ns, non-significant; Q2W, once every 2 weeks; Q4W, once every 4 weeks.

levels of *LDHA* expression during embryonic development between mice and humans, GalNAc-conjugated siRNAs are unable to penetrate the placenta to reach developing embryos. Correspondingly, we have demonstrated that liver-specific reduction of LDH with LDHA-1 treatment does not affect pregnancy, litter size, or survival to maturity in female wild-type mice (Figure S17).

In summary, our preclinical research clearly demonstrates that liver-specific suppression of LDH is efficacious in mouse models of PH1 and PH2, and shows the expected pharmacological activity in NHPs. By utilizing RNAi as a means to dissect the glyoxylate metabolic pathway in animal models, we have demonstrated that hepatic LDH is the key enzyme for oxalate production in all evaluated models of PH.

MATERIALS AND METHODS

Selection of Lead siRNAs

LDHA-1 and LDHA-2 siRNAs were identified through a process of large-scale screening of siRNAs for mRNA knockdown activity *in vitro* in HeLa cells (data not shown). RNA strands for siRNA duplexes were synthesized purified at Integrated DNA Technologies (Coralville, IA, USA). The final siRNA-GalNAc conjugates had a 36/22-mer duplex RNA structure, with a 36-nt sense strand composed of modified RNA and GalNAc conjugation that was annealed to a 22-nt modified RNA antisense strand. The siRNAs were modified with either 2′-OMe or 2′-F on their sugar moieties. *In vivo* ED_{50}s were determined in 6-week-old female CD-1 mice expressing endogenous mouse or exogenous human *LDHA* genes via s.c. injection. The lead HAO1-1 siRNA identified previously was conjugated with GalNAc and evaluated in 6-week-old female CD-1 mice.

siRNAs for *Grhpr*, *Hypdh*, *Hoga*, and *Agxt* were identified through a similar but smaller-scale screening process. After confirmation of activity in CD-1 mice, *Grhpr*, *Hypdh*, and *Hoga* siRNAs were used for mouse proof-of-concept studies. A second *Grhpr* siRNA was conjugated with GalNAc and evaluated in CD-1 mice for further proof-of-concept studies. *Agxt1* siRNA, formulated in LNP, was tested for suppression of AGT protein in male C57BL/6 mice following a single IV injection.

Mouse Models and *In Vivo* Testing

All animal experiments complied with the animal protocols approved by Dicerna's Institutional Animal Care and Use Committee. Mice were kept in a pathogen-free facility, with free access to standard chow (Picolab Rodent Diet 20; Lab Supply, Fort Worth, TX, USA) and water unless otherwise noted. CD-1 mice (Charles River

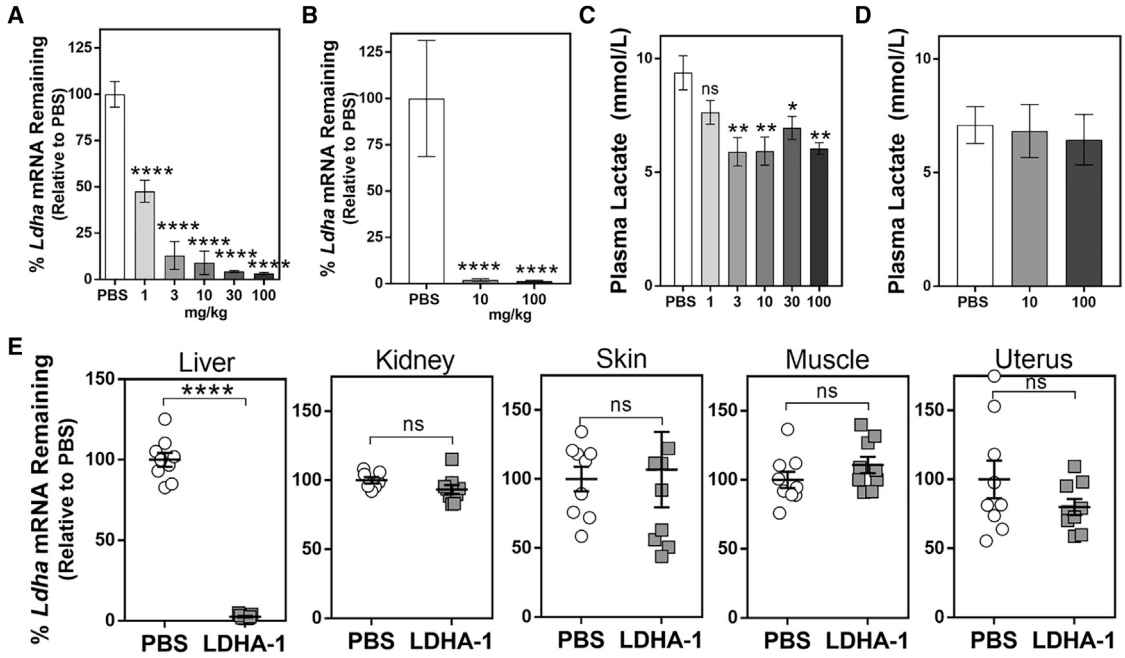

Figure 8. Study of Short-Term Liver-Specific Inhibition of *Ldha* in Mice

Wild-type and *Agxt1*$^{-/-}$ mice were given six weekly doses of LDHA-1 at the indicated dose levels. Blood samples along with liver, kidney, and skin tissue samples were collected 24 hr after the final dose. (A) *Ldha* mRNA expression measured by RT-PCR analysis in wild-type mice. Each group contains five animals. (B) *Ldha* mRNA expression measured by RT-PCR analysis in *Agxt1*$^{-/-}$ mice. Each group contained three male and three female animals. Plasma lactate was analyzed in (C) wild-type or (D) *Agx1t*$^{-/-}$ mice at different dose levels of LDHA-1. (E) Expression of *Ldha* mRNA was analyzed in liver, kidney, skin, and uterus of female *Agxt1*$^{-/-}$ mice treated with five weekly doses of LDHA-1 at 5 mg/kg. Expression level in each individual animal was analyzed. Data are presented as mean ± SD. One-way ANOVA (A–D) or unpaired t test (E) for statistical significance relative to PBS treatment group. *$p < 0.05$; **$p < 0.01$; ****$p < 0.0001$. ns, non-significant.

Laboratories, Wilmington, MA, USA) were used for *in vivo* screening of siRNA activity. C57BL/6 mice (Harlan Laboratories, Indianapolis, IN, USA) were used for testing the efficacy of lead siRNA conjugates.

For evaluating the effects of *Ldha* inhibition on lactate production in the muscle, we treated female CD-1 mice with four weekly doses of LDHA-1 and subjected them to a treadmill endurance test using a Panlab treadmill, model LE8708TS (Harvard Apparatus, Holliston, MA, USA). After conditioning on the treadmill, the study was initiated at a speed of 15 cm/s and a 10% incline. Treadmill speed was increased by approximately 3 cm/s every 3 min to a maximum speed of 38 cm/s until the mice were exhausted, which is defined by delayed response to 1.5 mA incentive stimulus imposed at the end of the treadmill. For one set of animals, approximately 10 μL blood samples were collected from the tail vein immediately, 5, 10, 30, or 60 min after exhaustion for analysis of lactate and pyruvate. A second set of animals was immediately sacrificed for blood and tissue collection.

Liver-specific targeting of LDHA-1 was assessed in female CD-1 mice during pregnancy. Female mice were pre-dosed with four weekly doses of LDHA-1, at which time they were mated to male CD-1 mice. Mice were visually observed and body weight measured to determine pregnancy status. Dosing continued until approximately 1 week before their anticipated delivery date. Immediately after delivery, litters were counted and all of the mothers sacrificed for tissue collection. The pups were sacrificed either immediately after birth or at time of full maturity (3 weeks of age) for mRNA analysis of liver tissue.

Agxt1$^{-/-}$ and *Grhpr*$^{-/-}$ mice were described previously.[24–28] *Agxt1*-, *Grhpr*-, or *Hoga1*-deficient mice were generated through a knockdown strategy utilizing siRNAs formulated in LNPs to reduce the expression of *Agxt1*, *Grhpr*, or *Hoga1* mRNA in C57BL/6 mice (Harlan Laboratories, Indianapolis, IN, USA). Dosing with PBS or siRNAs was done via s.c. injection for GalNAc-conjugated siRNAs or via intravenous injection for siRNAs in LNPs. EG was purchased from Sigma-Aldrich (St. Louis, MO, USA). In EG studies, mice were given free access to drinking water containing 0.7%, 1.4%, or 2.8% EG. Urine samples for all studies were collected manually or for approximately 18 hr using metabolic cages. Urine was acidified before analysis using previously published methods.[26,27] *Agxt1* knockdown mice were also subjected to hydroxyproline feeding. Mice were given free access to a custom animal diet (Research Diets, New Brunswick, NJ, USA) containing 1% hydroxyproline (Sigma-Aldrich, St. Louis, MO, USA). Urine samples from mice fed control versus hydroxyproline diet was measured for hydroxyproline content using a Hydroxyproline Assay Kit (Sigma-Aldrich, St. Louis, MO, USA) according to the manufacturer's instructions. Due to the

extremely low levels of hydroxyproline in most of the samples, absolute concentration of hydroxyproline could not be accurately calculated. Instead, absorbance values at 560 nm were compared.

Humanized liver mice (PXB mice) were purchased from PhoenixBio.[29] In brief, cDNA-urokinase-type plasminogen activator (uPA)/severe combined immunodeficiency (SCID) mice were transplanted with human hepatocytes (approximately 80% replacement). Transplant levels are calculated from measurement of blood human-albumin levels.

Blood Collections and Analysis

Terminal blood collections in mice were collected by cardiac puncture and processed to plasma using K_2EDTA or to serum using serum clot activator MiniCollect Plasma and Serum Tubes (Greiner Bio-One, Kremsmünster, Austria). Circulating alanine aminotransferase, aspartate aminotransferase, and alkaline phosphatase were measured by IDEXX BioResearch Laboratories (Grafton, MA, USA) using their established protocols.

Western Blot

Tissue lysates were prepared using TissueLyser II (QIAGEN, Valencia, CA, USA) with T-PER Tissue Protein Extraction Reagent and protease inhibitor cocktail (Thermo Fisher Scientific, Waltham, MA, USA). Total protein concentration was measured by BCA Protein Assay (Thermo Fisher Scientific, Waltham, MA, USA), and equal protein concentrations were resolved by NuPAGE 4%–12% Bis-Tris SDS-PAGE (Thermo Fisher Scientific, Waltham, MA, USA). Electrophoresed proteins were transferred to nitrocellulose membranes using the iBlot Dry Blotting System (Thermo Fisher Scientific, Waltham, MA, USA) and blocked with Odyssey Blocking Buffer (PBS) (Li-Cor Biosciences, Lincoln, NE, USA). Membranes were then incubated with rabbit anti-GO, rabbit anti-LDHA (Cell Signaling Technology, Danvers, MA, USA), rabbit anti-HYPDH (Abcam, Cambridge, MA, USA), or rabbit anti-AGT (Abcam, Cambridge, MA, USA) and with mouse anti-glyceraldehyde 3-phosphate dehydrogenase antibody (Abcam, Cambridge, MA, USA). Anti-rabbit IRDye 680 and anti-mouse IRDye 800 secondary antibodies (Li-Cor Biosciences, Lincoln, NE, USA) were used for detection, and signal intensity was measured using the Odyssey Infrared Imaging System (Li-Cor Biosciences, Lincoln, NE, USA).

RNA Preparation and Real-Time PCR

Tissue samples preserved in RNAlater (Thermo Fisher Scientific, Waltham, MA, USA) were homogenized in QIAzol Lysis Reagent using TissueLyser II (QIAGEN, Valencia, CA, USA). RNA was then purified using MagMAX Technology according to manufacturer's instructions (Thermo Fisher Scientific, Waltham, MA, USA). High-capacity cDNA reverse transcription kit (Thermo Fisher Scientific, Waltham, MA, USA) was used to prepare cDNA. Mouse-specific, NHP-specific, or human-specific *HAO1*, *LHDA*, *Grhpr*, *Hypdh*, *Hoga*, *Agxt*, and *Hprt1* primers (Integrated DNA Technology, Coralville, IA, USA) were used for PCR on a CFX384 Real-Time PCR Detection System (Bio-Rad Laboratories, Hercules, CA, USA).

Histological and Immunohistochemistry Analysis

Tissue were fixed in 10% neutral-buffered formalin overnight and then transferred to 70% ethanol. Embedding in paraffin and slide preparation as well as staining of tissues with H&E or Pizzolato's staining for CaOx were completed at Mass Histology Service (Worcester, MA, USA). For immunohistochemistry (IHC) experiments, paraffin sections were deparaffinized, rehydrated, and subjected to heat-mediated antigen retrieval (citrate buffer [pH 6.0]). Endogenous peroxidases were blocked with BLOXALL endogenous peroxidase and alkaline phosphatase blocking solution (Vector Laboratories, Burlingame, CA, USA) for 10 min. Rabbit polyclonal anti-LDHA antibody (1:50 dilution; Cell Signaling Technology, Danvers, MA, USA) was diluted in SignalStain Antibody Diluent (Cell Signaling Technology, Danvers, MA, USA) and incubated overnight at 4°C. Binding of the primary antibody was detected using a goat anti-rabbit IgG HRP antibody (Antibodies-online, Atlanta, GA, USA) and SignalStain DAB Substrate Kit (Cell Signaling Technology, Danvers, MA, USA). Results were visualized using an Olympus BX51 or a Nikon Eclipse Ti microscope and an OlympusBX61VS slide scanner using Image Pro Premier 9.1, NIS-Elements BR3.2, and Olympus VS-ASW image analysis software, respectively.

Histopathology analysis was conducted by a certified veterinary pathologist at IDEXX BioResearch Laboratories (West Sacramento, CA, USA).

LDH Enzyme Activity and Plasma Lactate and Pyruvate Assays

LDH enzyme activity in liver homogenates was measured using the Lactate Dehydrogenase Assay Kit (Colorimetric; Abcam, Cambridge, MA, USA) according to the manufacturer's instructions. Tissue lysates were prepared using TissueLyser II (QIAGEN, Valencia, CA, USA) with either LDH Assay Buffer or T-PER Tissue Protein Extraction Reagent and protease inhibitor cocktail (Thermo Fisher Scientific, Waltham, MA, USA). Total protein concentration was measured by BCA Protein Assay (Thermo Fisher Scientific, Waltham, MA, USA) and normalized concentrations used for LDH assay. Lactate and pyruvate levels in plasma samples were assessed using the L-Lactate and Pyruvate Assay Kits (Abcam, Cambridge, MA, USA) according to the manufacturer's instructions.

Enzymatic Oxalate Analysis and Creatinine Assay

Urine oxalate was measured using a clinical oxalate oxidase assay (Trinity Biotech, Wicklow, Ireland) modified for use with murine samples. Urine creatinine was measured using a standard creatinine detection kit (Enzo Life Sciences, Lausen, Switzerland).

LC/MS Method for Oxalate and Glycolate Measurement

Oxalate and glycolate were determined by methods based on liquid chromatography combined with mass spectrometry (MS) detection (LC/MS) on a triple-quadrupole instrument (API 5500; AB Sciex, Framingham, MA, USA) by electrospray ionization (ESI) and multiple reaction monitoring. Mouse and NHP urine samples were analyzed for oxalate and glycolate after sample dilution by hydrophilic interaction liquid chromatography and MS detection in

the negative ESI mode. Glycolate was determined in NHP plasma samples by protein precipitation, followed by chemical derivatization and analysis by reverse-phase LC and MS detection in the positive ESI mode. Stable-label internal standards ($^{13}C_2$-oxalate and $^{13}C_2$-glycolate) were utilized for quantification. Calibration curves were made in surrogate matrix. Quality-control samples were analyzed in triplicates at a minimum of three concentration levels in each analytical batch. The observed inaccuracy (%Bias) and precision (%CV [coefficient of variation]) for quality-control samples were less than 15% for all analyses.

NHP Study

Treatment of the animals was conducted by a certified contract research organization in accordance with the testing facility's standard operating procedure, which adheres to the regulations outlined in the US Department of Agriculture Animal Welfare Act (9 CFR, Parts 1–3) and the conditions specified in the Guide for the Care and Use of Laboratory Animals (ILAR publication, 1996, National Academy Press). Animals were given s.c. injections of siRNA in the interscapular region at the indicated time points. Dose administration and blood sample collection were conducted utilizing alert animals restrained in a primate produce restrainer system. Animals were fasted overnight (for a minimum of 12 hr) prior to the first scheduled blood collection on a given day. Blood samples were collected into serum separator tubes or EDTA tubes for preparation of serum and plasma, respectively. Blood sample and liver biopsy collections were scheduled relative to the end of the test article administration (±1.0 hr). At time points with liver biopsy and blood sample collection, animals were alert sampled prior to sedation for liver biopsy. For liver biopsies, animals were sedated with Telazol (4–6 mg/kg) and supplemented with ketamine (approximately 5 mg/kg). A percutaneous liver biopsy sample (approximately 20 mg of tissue) was collected. The sample was split in half for preservation in RNAlater (Thermo Fisher Scientific, Waltham, MA) or frozen at −70°C. For urine collections, animals were fasted and a urine collection pan was placed beneath the animal cage overnight. Urine samples were obtained in the morning before feeding. The volume of urine was recorded and the sample kept frozen at −70°C prior to analysis.

Statistical Analysis

Data are presented in graphs prepared using GraphPad Prism 7.02 (GraphPad Software, La Jolla, CA, USA) as mean ± SD. One-way ANOVA followed by Dunnett's multiple comparisons test or unpaired t tests were run using GraphPad Prism 7.02. Statistical significance is denoted as asterisks on the graphs (*$p < 0.05$; **$p < 0.01$; ***$p < 0.001$; ****$p < 0.0001$).

SUPPLEMENTAL INFORMATION

Supplemental Information includes seventeen figures and can be found with this article online at https://doi.org/10.1016/j.ymthe.2018.05.016.

AUTHOR CONTRIBUTIONS

C.L., N.P., and B.D.B. conceived and designed experiments; N.P., J.G., U.S., W.Z., M.D., R.D., C.D., M.K., C.M.-H., and E.S. performed the experiments; N.P., J.G., U.S., M.A., and H.D. analyzed the data; N.N., R.S., B.K., and W.W. contributed reagents/material/analysis tools; C.L., N.P., E.S., and B.D.B. wrote the manuscript.

CONFLICTS OF INTEREST

C.L., N.P., J.G., U.S., W.Z., M.D., R.D., C.D., M.K., N.N., R.S., B.K., W.W., M.A., H.D., and B.D.B. are or were employees of Dicerna Pharmaceuticals, which is developing siRNAs as therapeutics.

ACKNOWLEDGMENTS

We thank Doug Fambrough, Ralf Rosskamp, David Miller, Jennifer Lockridge, and Jim Weissman for their review of this manuscript. E.S. and C.M.-H. are partially supported by grant SAF2015-69796 from the Spanish Ministry of Science.

REFERENCES

1. Cochat, P., Hulton, S.A., Acquaviva, C., Danpure, C.J., Daudon, M., De Marchi, M., Fargue, S., Groothoff, J., Harambat, J., Hoppe, B., et al.; OxalEurope (2012). Primary hyperoxaluria Type 1: indications for screening and guidance for diagnosis and treatment. Nephrol. Dial. Transplant. *27*, 1729–1736.

2. Cochat, P., and Rumsby, G. (2013). Primary hyperoxaluria. N. Engl. J. Med. *369*, 649–658.

3. Danpure, C.J., and Rumsby, G. (2004). Molecular aetiology of primary hyperoxaluria and its implications for clinical management. Expert Rev. Mol. Med. *6*, 1–16.

4. Leumann, E., and Hoppe, B. (2001). The primary hyperoxalurias. J. Am. Soc. Nephrol. *12*, 1986–1993.

5. Martin-Higueras, C., Torres, A., and Salido, E. (2017). Molecular therapy of primary hyperoxaluria. J. Inherit. Metab. Dis. *40*, 481–489.

6. Zhao, F., Bergstralh, E.J., Mehta, R.A., Vaughan, L.E., Olson, J.B., Seide, B.M., Meek, A.M., Cogal, A.G., Lieske, J.C., and Milliner, D.S.; Investigators of Rare Kidney Stone Consortium (2016). Predictors of incident ESRD among patients with primary hyperoxaluria presenting prior to kidney failure. Clin. J. Am. Soc. Nephrol. *11*, 119–126.

7. Rumsby, G., and Hulton, S.A. (2008). Primary Hyperoxaluria Type 2. In GeneReviews, M.P. Adam, H.H. Ardinger, R.A. Pagon, and S.E. Wallace, eds. (University of Washington), https://www.ncbi.nlm.nih.gov/books/NBK1116/.

8. Salido, E., Pey, A.L., Rodriguez, R., and Lorenzo, V. (2012). Primary hyperoxalurias: disorders of glyoxylate detoxification. Biochim. Biophys. Acta *1822*, 1453–1464.

9. Hulton, S.A. (2016). The primary hyperoxalurias: a practical approach to diagnosis and treatment. Int. J. Surg. *36*, 649–654.

10. Monico, C.G., Rossetti, S., Belostotsky, R., Cogal, A.G., Herges, R.M., Seide, B.M., Olson, J.B., Bergstrahl, E.J., Williams, H.J., Haley, W.E., et al. (2011). Primary hyperoxaluria type III gene HOGA1 (formerly DHDPSL) as a possible risk factor for idiopathic calcium oxalate urolithiasis. Clin. J. Am. Soc. Nephrol. *6*, 2289–2295.

11. Milliner, D.S., Harris, P.C., and Lieske, J.C. (1993). Primary hyperoxaluria type 3. In GeneReviews, M.P. Adam, H.H. Ardinger, R.A. Pagon, and S.E. Wallace, eds. (University of Washington), https://www.ncbi.nlm.nih.gov/books/NBK316514/.

12. Poore, R.E., Hurst, C.H., Assimos, D.G., and Holmes, R.P. (1997). Pathways of hepatic oxalate synthesis and their regulation. Am. J. Physiol. *272*, C289–C294.

13. Mdluli, K., Booth, M.P., Brady, R.L., and Rumsby, G. (2005). A preliminary account of the properties of recombinant human Glyoxylate reductase (GRHPR), LDHA and LDHB with glyoxylate, and their potential roles in its metabolism. Biochim. Biophys. Acta *1753*, 209–216.

14. Smith, L.H., Jr., Bauer, R.L., Craig, J.C., Chan, R.P., and Williams, H.E. (1972). Inhibition of oxalate synthesis: in vitro studies using analogues of oxalate and glycolate. Biochem. Med. *6*, 317–332.

15. Williams, H.E., and Smith, L.H., Jr. (1971). Hyperoxaluria in L-glyceric aciduria: possible pathogenic mechanism. Science *171*, 390–391.

16. Markert, C.L., Shaklee, J.B., and Whitt, G.S. (1975). Evolution of a gene. Multiple genes for LDH isozymes provide a model of the evolution of gene structure, function and regulation. Science *189*, 102–114.

17. Doherty, J.R., and Cleveland, J.L. (2013). Targeting lactate metabolism for cancer therapeutics. J. Clin. Invest. *123*, 3685–3692.

18. Kanno, T., Sudo, K., Maekawa, M., Nishimura, Y., Ukita, M., and Fukutake, K. (1988). Lactate dehydrogenase M-subunit deficiency: a new type of hereditary exertional myopathy. Clin. Chim. Acta *173*, 89–98.

19. Kanno, T., Sudo, K., Takeuchi, I., Kanda, S., Honda, N., Nishimura, Y., and Oyama, K. (1980). Hereditary deficiency of lactate dehydrogenase M-subunit. Clin. Chim. Acta *108*, 267–276.

20. Takahashi, Y., Miyajima, H., and Kaneko, E. (1995). Genetic analysis of a family of lactate dehydrogenase A subunit deficiency. Intern. Med. *34*, 326–329.

21. Takayasu, S., Fujiwara, S., and Waki, T. (1991). Hereditary lactate dehydrogenase M-subunit deficiency: lactate dehydrogenase activity in skin lesions and in hair follicles. J. Am. Acad. Dermatol. *24*, 339–342.

22. Tsujino, S., Shanske, S., Brownell, A.K., Haller, R.G., and DiMauro, S. (1994). Molecular genetic studies of muscle lactate dehydrogenase deficiency in white patients. Ann. Neurol. *36*, 661–665.

23. Yoshikuni, K., Tagami, H., Yamada, M., Sudo, K., and Kanno, T. (1986). Erythematosquamous skin lesions in hereditary lactate dehydrogenase M-subunit deficiency. Arch. Dermatol. *122*, 1420–1424.

24. Dutta, C., Avitahl-Curtis, N., Pursell, N., Larsson Cohen, M., Holmes, B., Diwanji, R., Zhou, W., Apponi, L., Koser, M., Ying, B., et al. (2016). Inhibition of glycolate oxidase with Dicer-substrate siRNA reduces calcium oxalate deposition in a mouse model of primary hyperoxaluria type 1. Mol. Ther. *24*, 770–778.

25. Liebow, A., Li, X., Racie, T., Hettinger, J., Bettencourt, B.R., Najafian, N., Haslett, P., Fitzgerald, K., Holmes, R.P., Erbe, D., et al. (2017). An investigational RNAi therapeutic targeting glycolate oxidase reduces oxalate production in models of primary hyperoxaluria. J. Am. Soc. Nephrol. *28*, 494–503.

26. Salido, E.C., Li, X.M., Lu, Y., Wang, X., Santana, A., Roy-Chowdhury, N., Torres, A., Shapiro, L.J., and Roy-Chowdhury, J. (2006). Alanine-glyoxylate aminotransferase-deficient mice, a model for primary hyperoxaluria that responds to adenoviral gene transfer. Proc. Natl. Acad. Sci. USA *103*, 18249–18254.

27. Martin-Higueras, C., Luis-Lima, S., and Salido, E. (2016). Glycolate oxidase is a safe and efficient target for substrate reduction therapy in a mouse model of primary hyperoxaluria type I. Mol. Ther. *24*, 719–725.

28. Knight, J., Holmes, R.P., Cramer, S.D., Takayama, T., and Salido, E. (2012). Hydroxyproline metabolism in mouse models of primary hyperoxaluria. Am. J. Physiol. Renal Physiol. *302*, F688–F693.

29. Tateno, C., Kawase, Y., Tobita, Y., Hamamura, S., Ohshita, H., Yokomichi, H., Sanada, H., Kakuni, M., Shiota, A., Kojima, Y., et al. (2015). Generation of novel chimeric mice with humanized livers by using hemizygous cDNA-uPA/SCID mice. PLoS ONE *10*, e0142145.

30. Adeva-Andany, M., López-Ojén, M., Funcasta-Calderón, R., Ameneiros-Rodríguez, E., Donapetry-García, C., Vila-Altesor, M., and Rodríguez-Seijas, J. (2014). Comprehensive review on lactate metabolism in human health. Mitochondrion *17*, 76–100.

31. Belostotsky, R., Seboun, E., Idelson, G.H., Milliner, D.S., Becker-Cohen, R., Rinat, C., Monico, C.G., Feinstein, S., Ben-Shalom, E., Magen, D., et al. (2010). Mutations in DHDPSL are responsible for primary hyperoxaluria type III. Am. J. Hum. Genet. *87*, 392–399.

32. Belostotsky, R., Pitt, J.J., and Frishberg, Y. (2012). Primary hyperoxaluria type III—a model for studying perturbations in glyoxylate metabolism. J. Mol. Med. (Berl.) *90*, 1497–1504.

33. Pitt, J.J., Willis, F., Tzanakos, N., Belostotsky, R., and Frishberg, Y. (2015). 4-Hydroxyglutamate is a biomarker for primary hyperoxaluria type 3. JIMD Rep. *15*, 1–6.

34. Riedel, T.J., Johnson, L.C., Knight, J., Hantgan, R.R., Holmes, R.P., and Lowther, W.T. (2011). Structural and biochemical studies of human 4-hydroxy-2-oxoglutarate aldolase: implications for hydroxyproline metabolism in primary hyperoxaluria. PLoS ONE *6*, e26021.

35. Riedel, T.J., Knight, J., Murray, M.S., Milliner, D.S., Holmes, R.P., and Lowther, W.T. (2012). 4-Hydroxy-2-oxoglutarate aldolase inactivity in primary hyperoxaluria type 3 and glyoxylate reductase inhibition. Biochim. Biophys. Acta *1822*, 1544–1552.

36. Li, X., Knight, J., Todd Lowther, W., and Holmes, R.P. (2015). Hydroxyproline metabolism in a mouse model of Primary Hyperoxaluria Type 3. Biochim. Biophys. Acta *1852*, 2700–2705.

37. Danpure, C.J. (1997). Variable peroxisomal and mitochondrial targeting of alanine: glyoxylate aminotransferase in mammalian evolution and disease. BioEssays *19*, 317–326.

38. Miyajima, H., Takahashi, Y., and Kaneko, E. (1995). Characterization of the glycolysis in lactate dehydrogenase-A deficiency. Muscle Nerve *18*, 874–878.

39. Miyajima, H., Takahashi, Y., and Kaneko, E. (1995). Characterization of the oxidative metabolism in lactate dehydrogenase A deficiency. Intern. Med. *34*, 502–506.

40. Veech, R.L. (1991). The metabolism of lactate. NMR Biomed. *4*, 53–58.

41. Heigenhauser, G.J., and Parolin, M.L. (1999). Role of pyruvate dehydrogenase in lactate production in exercising human skeletal muscle. Adv. Exp. Med. Biol. *474*, 205–218.

42. Merkle, S., Favor, J., Graw, J., Hornhardt, S., and Pretsch, W. (1992). Hereditary lactate dehydrogenase A-subunit deficiency as cause of early postimplantation death of homozygotes in Mus musculus. Genetics *131*, 413–421.

43. Pretsch, W., Merkle, S., Favor, J., and Werner, T. (1993). A mutation affecting the lactate dehydrogenase locus Ldh-1 in the mouse. II. Mechanism of the LDH-A deficiency associated with hemolytic anemia. Genetics *135*, 161–170.

44. Fieldhouse, B., and Masters, C.J. (1966). Developmental redistributions of porcine lactate dehydrogenase. Biochim. Biophys. Acta *118*, 538–548.